Matching-pursuit/split-operator Fourier-transform simulations of nonadiabatic quantum dynamics

Yinghua Wu and Michael F. Herman
Department of Chemistry, Tulane University, 6400 Freret Street, New Orleans, Louisiana 70118

Victor S. Batista[a)]
Department of Chemistry, Yale University, P.O. Box 208107, New Haven, Connecticut 06520-8107

(Received 18 January 2005; accepted 3 February 2005; published online 24 March 2005)

A rigorous and practical approach for simulations of nonadiabatic quantum dynamics is introduced. The algorithm involves a natural extension of the matching-pursuit/split-operator Fourier-transform (MP/SOFT) method [Y. Wu and V. S. Batista, J. Chem. Phys. **121**, 1676 (2004)] recently developed for simulations of adiabatic quantum dynamics in multidimensional systems. The MP/SOFT propagation scheme, extended to nonadiabatic dynamics, recursively applies the time-evolution operator as defined by the standard perturbation expansion to first-, or second-order, accuracy. The expansion is implemented in dynamically adaptive coherent-state representations, generated by an approach that combines the matching-pursuit algorithm with a gradient-based optimization method. The accuracy and efficiency of the resulting propagation method are demonstrated as applied to the canonical model systems introduced by Tully for testing simulations of dual curve-crossing nonadiabatic dynamics. © *2005 American Institute of Physics*. [DOI: 10.1063/1.1881132]

I. INTRODUCTION

Nonadiabatic quantum dynamics is a ubiquitous phenomenon in physical, chemical, and biological processes.[1,2] Describing nonadiabatic quantum dynamics at the most fundamental level of theory, however, requires solving the coupled system of differential equations defined by the time-dependent Schrödinger equation. In recent years, much effort has been devoted to the development of numerically exact methods[3–15] for wave-packet propagation based on the split-operator Fourier-transform (SOFT) approach,[16–18] the Chebyshev expansion,[19] and the short iterative Lanczos[20] algorithms. While rigorous, these approaches are limited to systems with very few degrees of freedom (e.g., molecular systems with less than 3 or 4 atoms) since they require storage space and computational effort that scale exponentially with the number of coupled degrees of freedom. Such an exponential scaling problem has limited studies of nonadiabatic dynamics in complex molecular systems to approximate methods built around semiclassical and mixed quantum-classical treatments.[21–35] However practical, these approximate approaches require a compromise between accuracy and feasibility and rely on *ad hoc* approximations whose resulting consequences are often difficult to quantify in applications to complex (nonintegrable) dynamics. It is, therefore, essential to develop practical methods for numerically exact simulations in order to validate approximate approaches and provide new insights into the nature of quantum processes. This paper describes an extension of the recently developed matching-pursuit/split-operator Fourier-transform (MP/SOFT) method[36–38] to simulations of nonadiabatic quantum dynamics. The accuracy and efficiency of the extended MP/ SOFT method are demonstrated as applied to benchmark simulations of dual curve-crossing dynamics.

The MP/SOFT method[36–38] has been recently introduced in an effort to develop a simple and rigorous time-dependent method for simulations of quantum processes in multidimensional systems. The MP/SOFT methodology is based on the recursive application of the time-evolution operator, as defined by the Trotter expansion to second-order accuracy, to nonorthogonal and dynamically adaptive coherent-state representations generated according to the matching-pursuit algorithm.[39] The main advantage of this approach relative to the standard grid-based SOFT method is that the coherent-state expansions allow for an *analytic* implementation of the Trotter expansion, bypassing the exponential scaling problem associated with the fast-Fourier-transform (FFT) algorithm of usual grid-based implementations. When compared to other time-dependent methods based on coherent-state expansions,[40–53] the MP/SOFT method has the advantage of avoiding the usual need of solving a coupled system of differential equations for propagating expansion coefficients. Further, the MP/SOFT method implements a successive orthogonal decomposition scheme that overcomes the usual numerical difficulties due to overcompleteness introduced by nonorthogonal basis functions.[7] The main drawback of the MP/SOFT method is that it requires generating a new coherent-state expansion of the time evolving state for each propagation step. However, the underlying computational task can be trivially parallelized.

To date, the capabilities of the MP/SOFT method have been demonstrated in application to simulations of adiabatic quantum dynamics, including simulations of tunneling dynamics in model systems with up to 20 coupled degrees of freedom.[38] In a recent development, the approach has been generalized to provide accurate descriptions of thermal-

[a)]Electronic mail: victor.batista@yale.edu

equilibrium density matrices, finite-temperature time-dependent expectation values, and time-correlation functions.[54] There remains, however, the nontrivial question as to whether the MP/SOFT methodology can be easily implemented to model nonadiabatic processes. This paper concludes the affirmative, that such a methodology can indeed be effectively applied to simulations of nonadiabatic dynamics simply by describing nonadiabaticity according to a short-time approximation of the time-evolution operator as defined by the perturbation expansion to first-, or second-order, accuracy. While the paper is focused only on validating the MP/SOFT methodology by performing rigorous comparisons with benchmark calculations for reduced-dimensional model systems, the results at least suggest the potential for application of the MP/SOFT method to the description of nonadiabatic dynamics in complex (i.e., nonintegrable) quantum dynamics.

This paper is organized as follows. Section II describes the extension of the MP/SOFT method to simulations of nonadiabatic quantum dynamics according to the successive implementation of the time-evolution operator, as defined by a time-dependent perturbation theory expansion. Section III presents the numerical results of a series of benchmark calculations of dual curve-crossing nonadiabatic dynamics simulations. Section IV summarizes and concludes.

II. METHODS

The generalization of the MP/SOFT method to nonadiabatic dynamics is based on the recursive application of the time-evolution operator as defined by the standard perturbation expansion,

$$e^{-i\hat{H}2\tau} = e^{-i\hat{H}_0 2\tau} - i\int_0^{2\tau} dt_1 e^{-i\hat{H}_0(2\tau-t_1)}\hat{H}_1 e^{-i\hat{H}_0 t_1} + (-i)^2\int_0^{2\tau} dt_2 \int_0^{t_2} dt_1 e^{-i\hat{H}_0(2\tau-t_2)}\hat{H}_1 \times e^{-i\hat{H}_0(t_2-t_1)}\hat{H}_1 e^{-i\hat{H}_0 t_1} + \cdots, \quad (1)$$

with τ a sufficiently short time increment for the evolution of the system according to the Hamiltonian

$$\hat{H} = \hat{H}_0 + \hat{H}_1, \quad (2)$$

where $\hat{H}_0$ and $\hat{H}_1$ are defined in the basis set of diabatic states (e.g., electronic states) as follows:

$$\hat{H}_0 = \frac{\hat{\mathbf{p}}^2}{2m} + \sum_{k=1}^{n} V_k(\hat{\mathbf{x}})|k\rangle\langle k|, \quad (3)$$

and

$$\hat{H}_1 = \sum_{k=1}^{n}\sum_{j\neq k}^{n} V_c(\hat{\mathbf{x}})|j\rangle\langle k|. \quad (4)$$

Note that the unperturbed Hamiltonian $\hat{H}_0$ describes the adiabatic dynamics of coordinates $\mathbf{x}$ (e.g., nuclear coordinates) on the uncoupled potential-energy surfaces $V_k(\mathbf{x})$, while the perturbation $\hat{H}_1$ introduces the nonadiabatic couplings $V_c(\mathbf{x})$ between potential-energy surfaces. To keep the notation as simple as possible, all expressions are written in mass-weighted coordinates and atomic units, so that all degrees of freedom have the same mass m and $\hbar=1$.

The perturbation expansion, introduced by Eq. (1), can be approximated for sufficiently small propagation time increments τ as follows:

$$e^{-i\hat{H}2\tau} \approx e^{-i\hat{H}_0 2\tau} - i2\tau e^{-i\hat{H}_0\tau}\hat{H}_1 e^{-i\hat{H}_0\tau} - 2\tau^2 e^{-i\hat{H}_0 2\tau/3}\hat{H}_1 e^{-i\hat{H}_0 2\tau/3}\hat{H}_1 e^{-i\hat{H}_0 2\tau/3} + \cdots, \quad (5)$$

where the first-order term in Eq. (1) has been evaluated according to the "midpoint" approximation (i.e., $t_1=\tau$) and the second-order term was evaluated according to the "center-of-mass" approximation (i.e., $t_1=2\tau/3$ and $t_2=4\tau/3$). The extension of the MP/SOFT method, introduced in this paper, recursively implements the time-evolution operator, as defined in Eq. (5), to first, or second, order.

In order to describe the MP/SOFT implementation of Eq. (5) to first-order accuracy, consider a two-level system ($n=2$) described by the time-dependent wave function,

$$|\Psi(\mathbf{x};t)\rangle = \varphi_1(\mathbf{x};t)|1\rangle + \varphi_2(\mathbf{x};t)|2\rangle, \quad (6)$$

where $\varphi_j(\mathbf{x};t)$ is the time-dependent wave-packet component associated with diabatic state $|j\rangle$. Note that generalizations to multiple-level systems, or higher order of perturbation theory (e.g., second-order accuracy), are straightforward.

The implementation of Eq. (5) to first order requires the following steps:

- Step [I]. Propagate the wave-packet components $\varphi_1(\mathbf{x};t)$ and $\varphi_2(\mathbf{x};t)$ adiabatically for time τ,

$$\varphi_1'(\mathbf{x};t+\tau) = e^{-i\left[\frac{\hat{\mathbf{p}}^2}{2m}+V_1(\hat{\mathbf{x}})\right]\tau}\varphi_1(\mathbf{x};t),$$

$$\varphi_2'(\mathbf{x};t+\tau) = e^{-i\left[\frac{\hat{\mathbf{p}}^2}{2m}+V_2(\hat{\mathbf{x}})\right]\tau}\varphi_2(\mathbf{x};t). \quad (7)$$

- Step [II]. Mix the two wave-packet components, $\varphi_1'(\mathbf{x};t+\tau)$ and $\varphi_2'(\mathbf{x};t+\tau)$,

$$\varphi_1''(\mathbf{x};t+\tau) = \varphi_1'(\mathbf{x};t+\tau) - i2\tau V_c(\mathbf{x})\varphi_2'(\mathbf{x};t+\tau),$$

$$\varphi_2''(\mathbf{x};t+\tau) = \varphi_2'(\mathbf{x};t+\tau) - i2\tau V_c(\mathbf{x})\varphi_1'(\mathbf{x};t+\tau). \quad (8)$$

- Step [III]. Propagate the mixed wave-packet components, $\varphi_1''(\mathbf{x};t+\tau)$ and $\varphi_2''(\mathbf{x};t+\tau)$, adiabatically for time τ,

$$\varphi_1(\mathbf{x};t+2\tau) = e^{-i\left[\frac{\hat{\mathbf{p}}^2}{2m}+V_1(\hat{\mathbf{x}})\right]\tau}\varphi_1''(\mathbf{x};t+\tau),$$

$$\varphi_2(\mathbf{x};t+2\tau) = e^{-i\left[\frac{\hat{\mathbf{p}}^2}{2m}+V_2(\hat{\mathbf{x}})\right]\tau}\varphi_2''(\mathbf{x};t+\tau). \quad (9)$$

  Step [III] is, however, combined with step [I] of the next propagation time sliced for all but the last propagation time increment.

The mixing of wave-packet components in step [II] can be implemented analytically whenever the couplings $V_c(\mathbf{x})$ are Gaussians (e.g., see the first two model systems in Sec. III) since φ_1' and φ_2' are coherent-state expansions [i.e., see

Eq. (11)]. In general, however, mixing the wave-packet components φ_1' and φ_2' requires expanding the target states φ_1'' and φ_2'' in matching-pursuit coherent-states expansions (*vide infra*).

Steps [I] and [III] involve the adiabatic propagation of the wave-packet components according to the MP/SOFT implementation of the Trotter expansion,

$$e^{-i\left[\frac{\hat{\mathbf{p}}^2}{2m}+V_1(\hat{\mathbf{x}})\right]\tau} \approx e^{-iV_i(\hat{\mathbf{x}})\tau/2} e^{-i\frac{\hat{\mathbf{p}}^2}{2m}\tau} e^{-iV_i(\hat{\mathbf{x}})\tau/2}, \tag{10}$$

as described in Ref. 38. Such an approach can be outlined as follows:

- Step [1]. Decompose the target functions $\varphi_l'(\mathbf{x};t) \equiv e^{-iV(\hat{\mathbf{x}})\tau/2}\varphi_l(\mathbf{x};t)$, where $l=1$, and 2, into a matching-pursuit coherent-state expansion,

$$\varphi_l'(\mathbf{x};t) \approx \sum_{j=1}^{n} c_j \langle \mathbf{x}|\chi_j\rangle. \tag{11}$$

  Here, $\langle \mathbf{x}|\chi_j\rangle$ are N-dimensional coherent states,

$$\langle \mathbf{x}|\chi_j\rangle \equiv \prod_{k=1}^{N} A_j(k) \exp\left\{ -\frac{\gamma_j(k)}{2}[x(k)-x_j(k)]^2 + ip_j(k)[x(k)-x_j(k)] \right\}, \tag{12}$$

  where $A_j(k)$ are normalization factors and $\gamma_j(k)$, $x_j(k)$, and $p_j(k)$ are complex-valued parameters selected according to the matching-pursuit algorithm, as described later in this section. The expansion coefficients c_j are defined as follows: $c_1 \equiv \langle \chi_1|\varphi_l'\rangle$ and $c_j \equiv \langle \chi_j|\varphi_l'\rangle - \sum_{k=1}^{j-1} c_k \langle \chi_j|\chi_k\rangle$ for $j=2-N$.

- Step [2]. Apply the kinetic part of the Trotter expansion to $\varphi_l'(\mathbf{x};t)$ by first Fourier transforming the coherent-state expansion of $\varphi_l'(\mathbf{x};t)$ to the momentum representation, then multiplying it by $\exp[-i(\mathbf{p}^2/2m)\tau]$, and finally inverse Fourier transforming the product back to the coordinate representation to obtain

$$\varphi_l''(\mathbf{x};t) = \sum_{j=1}^{n} c_j \langle \mathbf{x}|\tilde{\chi}_j\rangle, \tag{13}$$

  where

$$\langle \mathbf{x}|\tilde{\chi}_j\rangle \equiv \prod_{k=1}^{N} A_j(k) \sqrt{\frac{m}{m+i\tau\gamma_j(k)}} \times \exp\left(\frac{\left\{ \frac{p_j(k)}{\gamma_j(k)} - i[x_j(k)-x(k)] \right\}^2}{\frac{2}{\gamma_j(k)} + \frac{2i\tau}{m}} - \frac{p_j(k)}{2\gamma_j(k)} \right). \tag{14}$$

  The time-evolved wave-function components are thus

$$\varphi_l(\mathbf{x};t+\tau) = \sum_{j=1}^{n} c_j e^{-iV(\mathbf{x})\tau/2} \langle \mathbf{x}|\tilde{\chi}_j\rangle, \tag{15}$$

  which can be reexpanded in coherent states, as in step [1].

Note that, since step [2] is implemented analytically, the underlying computational task necessary for nonadiabatic propagation is completely reduced to generating the coherent-state expansions introduced in Eq. (11) and in the mixing step.

Coherent-state expansions are obtained by combining the matching-pursuit algorithm with a gradient-based optimization technique as follows:

- Step [1.1]. Starting from an initial trial coherent state $|\chi_j\rangle$, optimize both the real and imaginary parts of the parameters $x_j(k)$, $p_j(k)$, and $\gamma_j(k)$ so that it locally maximizes the overlap with the target state $|\varphi_l'(t)\rangle$. Note that coherent-state parameters $\gamma_j(k)$, $x_j(k)$, and $p_j(k)$ are initially chosen as defined by the basis elements of previous representations (or the initial state) and are allowed to locally relax according to a steepest-descent optimization process. The state $|\chi_1\rangle$ that locally maximizes the overlap with the target state is the first basis function in the expansion on which the target state is projected as follows:

$$|\varphi_l'(t)\rangle = c_1|\chi_1\rangle + |\varepsilon_1\rangle, \tag{16}$$

  where $c_1 \equiv \langle \chi_1|\varphi_l'(t)\rangle$ and ε_1 is the residue after the first expansion. Note that ε_1 is orthogonal to $|\chi_1\rangle$ due to the definition of c_1.

- Step [1.2]. Replacing the target state by ε_1, go to step [1.1] to subdecompose ε_1 by its locally optimum match $|\chi_2\rangle$ as follows:

$$|\varepsilon_1\rangle = c_2|\chi_2\rangle + |\varepsilon_2\rangle, \tag{17}$$

  where $c_2 \equiv \langle \chi_2|\varepsilon_2\rangle$. Similarly, $|\chi_2\rangle$ is orthogonal to $|\varepsilon_1\rangle$ and hence, $|\varepsilon_2| \leqslant |\varepsilon_1|$.

Step [1.2] is repeated each time on the following residue. After n successive orthogonal projections, the norm of the residue is smaller than a desired precision ε,

$$|\varepsilon_n| = \sqrt{1-\sum_{j=1}^{n} c_j^2} \leqslant \varepsilon, \tag{18}$$

and the resulting expansion is obtained.

Note that the propagation scheme described in this section is a natural generalization of the method described in Ref. 38, since in the limiting case of adiabatic quantum dynamics [i.e., $V_c(\mathbf{x})=0$] the two methods are identical. It is important to mention, however, that since the extension to nonadiabatic dynamics involves a perturbation expansion that does not conserve the norm of the wave packet, the results may need to be renormalized at any desired time according to the corresponding level of perturbation theory.

III. RESULTS

This section demonstrates the capabilities of the generalized MP/SOFT propagation scheme, introduced in Sec. II, as applied to the canonical model systems introduced by Tully to test dual curve-crossing nonadiabatic dynamics.[22] These models are particularly suitable for benchmark calculations since they have been widely implemented in tests of other propagation methods for simulations of nonadiabatic dynamics, including approaches based on coherent-state representations.[25,55] The propagation scheme is still basically a coherent-state version of the SOFT approach in the spirit of the original formulation, which has already been shown to be accurate in earlier studies.[36–38] Therefore, the simulations performed in this paper are essentially tests on the time-dependent perturbation approximation as applied to different nonadiabatic coupling models.

The first model is an example of weak coupling and involves single avoided crossing dynamics. The second and third models involve dual avoided crossing and extended coupling, representing medium and strong coupling cases, respectively. Details of the model systems are readily available in Ref. 22 and will not be discussed here.

The initial wave packet represents a particle of mass of 2000 amu. It is prepared to the left of the coupling region, with some initial momentum in the rightward direction and starts on the lower diabatic potential-energy surface. Specifically, the initial wave function is chosen to be Gaussian with the two components in Eq. (6) defined as

$$\varphi_1(\mathbf{x};0) = \left(\frac{\gamma}{\pi}\right)^{1/4} e^{-(\gamma/2)(x-x_0)^2 + ip_0(x-x_0)},$$

$$\varphi_2(\mathbf{x};0) = 0, \tag{19}$$

where p_0 is the initial momentum and $\gamma = p_0^2/200$. Thus the initial wave packet has an energy spread of about $\pm 10\%$ of its energy, as in Ref. 22.

The simulations of nonadiabatic dynamics, based on the method introduced in Sec. II, are compared to full quantum-mechanical calculations obtained according to the standard grid-based SOFT approach.[16–18] Performance is measured by examining the transmission and reflection probabilities $P_k^{(T)}$ and $P_k^{(R)}$, as a function of the initial momentum p_0 (i.e., kinetic energy). Here, the labels $k=1$ and 2 correspond to the two diabatic states $|1\rangle$ and $|2\rangle$, respectively. The transmission and reflection probabilities are obtained as follows:

$$P_k^{(T)} = \lim_{t\to\infty} \int_0^\infty dx \varphi_k(\mathbf{x};t)^* \varphi_k(\mathbf{x};t), \tag{20}$$

and

$$P_k^{(R)} = \lim_{t\to\infty} \int_{-\infty}^0 dx \varphi_k(\mathbf{x};t)^* \varphi_k(\mathbf{x};t). \tag{21}$$

Excellent agreement between MP/SOFT and benchmark grid-based calculations is demonstrated for all three model systems investigated. Results are obtained with rather efficient coherent-state representations, usually including fewer than 50 coherent states ($n \leqslant 50$). The results are shown to be independent of the integration time interval τ so long as τ is chosen to be sufficiently small.

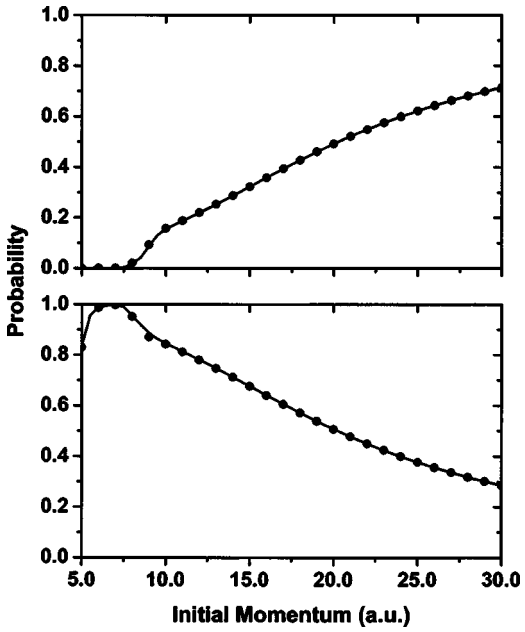

FIG. 1. Transmission probabilities $P_1^{(T)}$ (upper panel) and $P_2^{(T)}$ (lower panel), as a function of the initial wave-packet momentum, for the single avoided crossing model introduced by Eq. (22). Benchmark quantum calculations (solid line) are compared to MP/SOFT results (filled circles) obtained according to the perturbation expansion to first-order accuracy, as described in the text.

A. Single avoided crossing

The first model defines a problem of single avoided crossing dynamics according to the following potential-energy surfaces and coupling functions defined in the diabatic representation:

$$V_1(x) = 0.01[1 - \exp(-1.6x)], \quad x > 0,$$

$$V_1(x) = -0.01[1 - \exp(1.6x)], \quad x < 0,$$

$$V_2(x) = -V_1(x),$$

$$V_c(x) = 0.005 \exp(-1.0x^2). \tag{22}$$

The initial wave packet is prepared, according to Eq. (19), centered at $x_0 = -8.0$ a.u. and with positive momentum $p_0 = 5$–30 a.u. The time-dependent Schrödinger equation is integrated until the wave packet completely leaves the interaction region and the transmission probabilities remain constant. Both sets of calculations involve the propagation of the initial wave packet for 3000 a.u., using an integration time increment $\tau = 10$ a.u. Benchmark quantum-mechanical calculations implement a grid of 8192 points, extended over the $x = -25.0$ to 50.0 a.u. range.

Figure 1 compares transmission probabilities $P_1^{(T)}$ (i.e., on the upper adiabatic state) and $P_2^{(T)}$ (i.e., on the lower adiabatic state), as a function of the initial wave-packet momentum. Results obtained according to the MP/SOFT method (filled circles), in conjunction with the perturbation expan-

sion to first-order accuracy, are compared to grid-based quantum-mechanical calculations (solid line).

Figure 1 shows that the generalized MP/SOFT method, introduced in Sec. II, is able to reproduce the description of single avoided crossing dynamics for the whole range of energy (i.e., initial momentum) investigated, in quantitative agreement with benchmark quantum-mechanical calculations.

B. Dual avoided crossing

The model for dual avoided crossing dynamics is defined in the diabatic representation according to the following potential-energy surfaces and coupling functions:

$$V_1(x) = 0,$$

$$V_2(x) = -0.1 \exp(-0.28x) + 0.05,$$

$$V_c(x) = 0.015 \exp(-0.06x^2). \tag{23}$$

The initial wave packet is prepared, according to Eq. (19), localized in the asymptotic negative region with $x_0 = -15.0$ a.u. and a positive momentum. The time-dependent Schrödinger equation is integrated until the wave packet completely leaves the interaction region and the transmission probability remains constant for all future times. Both sets of calculations involved propagation of the initial wave packet for 3000 a.u., using an integration time increment $\tau = 1$ a.u. Benchmark calculations implemented a grid of 8192 points, extended in the $x = -35.0$ to 35.0 a.u. range. While the strength of the couplings demanded a rather small propagation time increment $\tau = 1$ a.u., the efficiency of the propagation scheme could in principle be further improved by implementing a variable time-step integrator as determined by the average strength of the nonadiabatic couplings and the initial momentum.

It is important to note that this dual avoided crossing model problem is significantly more challenging for a perturbational approach than the single avoided crossing model discussed in Sec. III A, since in this case the coupling amplitudes and the range of the couplings are larger. Furthermore, the model involves dual avoided crossing dynamics with quantum interferences between the two crossings manifesting Stuckelberg oscillations.[56]

Figure 2 compares transmission probabilities $P_1^{(T)}$ (i.e., on the upper adiabatic state) and $P_2^{(T)}$ (i.e., on the lower adiabatic state), as a function of the initial wave-packet momentum. Results obtained according to the MP/SOFT method (filled circles), in conjunction with the perturbation expansion to first-order accuracy, are compared to grid-based quantum-mechanical calculations (solid line). The comparison shows that, once again, the results obtained according to the generalized MP/SOFT method agree quantitatively with benchmark quantum-mechanical calculations throughout the entire range of energy (i.e., initial momentum) considered. Note especially that the oscillatory transmission probabilities are reproduced in excellent agreement with benchmark calculations, even at low energies that have defied other methods based on coherent-state representations.[25]

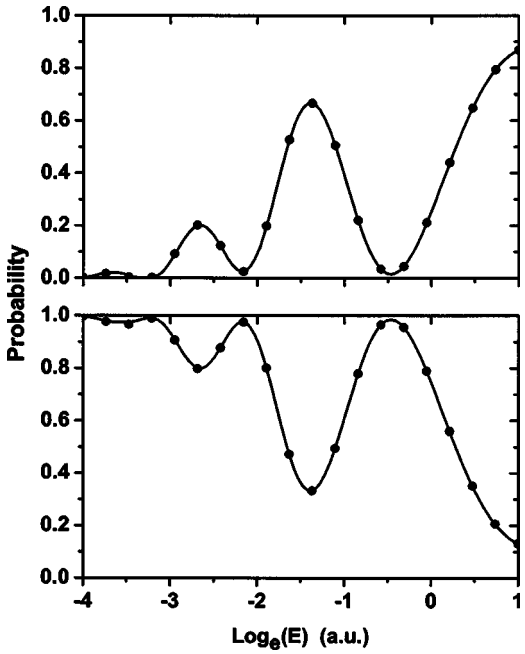

FIG. 2. Transmission probabilities $P_1^{(T)}$ (upper panel) and $P_2^{(T)}$ (lower panel), as a function of the initial wave-packet momentum, for the dual avoided crossing model, introduced by Eq. (23). Benchmark quantum calculations (solid line) are compared to MP/SOFT results (filled circles) obtained according to the perturbation expansion to first-order accuracy, as described in the text.

In order to show that the agreement between MP/SOFT and benchmark calculations applies not only to the long-time asymptotic state but also to all intermediate times during the scattering event, Fig. 3 shows the time-dependent populations of both adiabatic states for a wave packet initially prepared in the asymptotic negative region with $x_0 = -15.0$ a.u. and $p_0 = 25.0$ a.u. The agreement between MP/SOFT and benchmark calculations indicates that the first-order perturbational scheme is able to successfully describe not only the Stuckelberg oscillations but also the detailed evolution of time-dependent populations as determined by the quantum-mechanical interferences due to the two curve crossings.

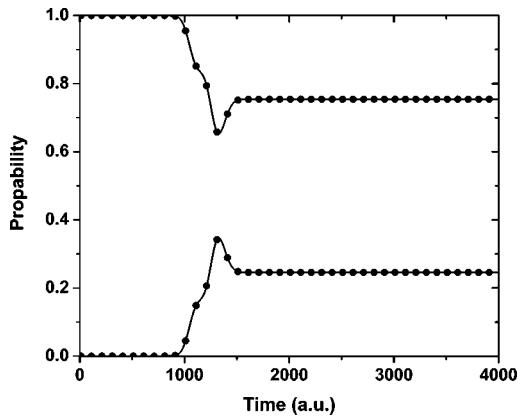

FIG. 3. Time-dependent populations of both adiabatic states for a wave packet initially prepared in the asymptotic negative region with $x_0 = -15.0$ a.u. and $p_0 = 25.0$ a.u. Benchmark quantum calculations (solid line) are compared to MP/SOFT results (filled circles), obtained according to the perturbation expansion to first-order accuracy, as described in the text.

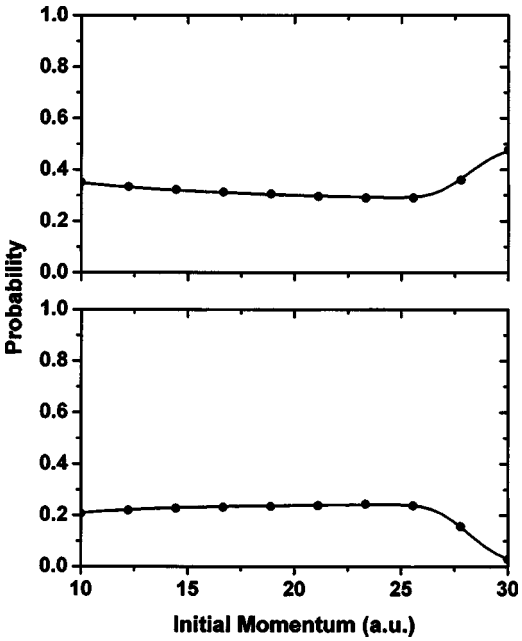

FIG. 4. Probabilities of transmission (upper panel) and reflection (lower panel), associated with the extended coupling with reflection model introduced by Eq. (24), for the upper diabatic state, as a function of the initial wave-packet momentum. Benchmark quantum calculations (solid line) are compared to MP/SOFT results (filled circles), obtained according to the second-order perturbation expansion, as described in the text.

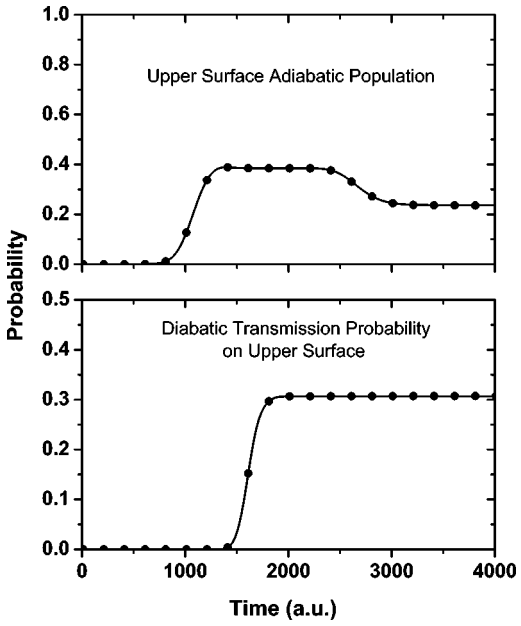

FIG. 5. Time-dependent populations of the upper adiabatic state (upper panel) and diabatic transmission probability on upper surface (lower panel) for the extended coupling with reflection model. The wave packet is initially prepared on the lowest-energy state (i.e., the first diabatic state) in the asymptotic negative region with $x_0=-15.0$ a.u. and $p_0=18.0$ a.u. Benchmark quantum calculations (solid line) are compared to MP/SOFT results (filled circles), obtained according to the perturbation expansion to second-order accuracy, as described in the text.

C. Extended coupling with reflection

The problem of extended coupling is an even more difficult test for the perturbational implementation of the MP/SOFT methodology. Here, the couplings between diabatic states do not go to zero in the asymptotic region. Furthermore, the coupling amplitudes and the range of couplings are even larger than in the previous models. The diabatic potentials are

$$V_2(x) = 6 \times 10^{-4}, \quad V_1(x) = -6 \times 10^{-4},$$

$$V_c(x) = 0.1 \exp(-0.9x), \quad x < 0,$$

$$V_c(x) = 0.1[2 - \exp(-0.9x)], \quad x > 0. \tag{24}$$

Since the diabatic states are close in energy, the transmission and reflection probabilities are very similar for both diabatic states. The adiabatic surfaces, on the other hand, show a barrier for the upper state and one would thus expect some reflection for energies below this barrier. All these effects are observed in the MP/SOFT calculations, in excellent agreement with benchmark quantum-mechanical results.

Figure 4 shows the transmission (upper panel) and reflection (lower panel) probabilities, associated with the extended coupling model introduced by Eq. (24), for the upper diabatic state as a function of the initial wave-packet momentum.

Results are obtained by preparing the initial wave packet centered at $x_0=-15.0$ a.u. and with positive momentum $p_0=10$–30 a.u. As before, the time-dependent Schrödinger equation is integrated until the transmission probabilities remain constant. Both sets of calculations involved propagation of the initial wave packet for 9000 a.u. Due to partial reflection, benchmark calculations without absorbing potentials required a rather large grid of 16 384 points extended over the $x=-150.0$ to 200.0 a.u. range.

Due to the strength and extension of the coupling potentials, accurate calculations based on the MP/SOFT method required a perturbation expansion to second-order accuracy and a rather small integration time increment $\tau=0.2$ a.u. Results were obtained, as described in Sec. II, by using the midpoint approximation for the first order term and the center-of-mass approximation in the evaluation of the second-order term in the perturbational expansion.

In order to show that the agreement between MP/SOFT and benchmark calculations is observed not only for the asymptotic states but also for all intermediate times during the scattering event, Fig. 5 shows the time-dependent populations of the diabatic and upper adiabatic states for a wave packet initially prepared on the lowest-energy state (i.e., the first diabatic state) in the asymptotic negative region with $x_0=-15.0$ a.u. and $p_0=18.0$ a.u. The agreement between MP/SOFT and benchmark calculations indicates that the second-order perturbational scheme is able to successfully describe not only the asymptotic transmission probabilities but also the detailed evolution of time-dependent populations as determined by the curves with extended couplings. For comparison, note that the MP/SOFT scheme to second-order accuracy in the perturbation expansion performs significantly better than other methods based on coherent-state expansions[25] and requires expansions with much fewer basis functions (e.g., $n \gtrsim 100$).

IV. CONCLUDING REMARKS

We have introduced a generalization of the MP/SOFT method to simulate nonadiabatic quantum dynamics. The method is both rigorous and practical and involves a propagation scheme that recursively applies the standard perturbation expansion of the time-evolution operator. The expansion is implemented in dynamically adaptive coherent-state representations, generated by an approach that combines the matching-pursuit algorithm with a gradient-based optimization method.

We have shown that the generalization of the method to nonadiabatic dynamics simulations still preserves the structure of the original MP/SOFT formulation, which is basically a coherent-state version of the SOFT approach. As mentioned in Refs. 36–38, the main advantage of the MP/SOFT approach relative to the standard grid-based SOFT method is that the coherent-state representations allow for an *analytic* evaluation of the Trotter expansion, bypassing the exponential scaling problem associated with the FFT algorithm of usual grid-based implementations. When compared to other time-dependent methods based on coherent-state expansions, the method developed here has the advantage of avoiding the usual need of propagating expansion coefficients by solving a coupled system of differential equations. The main drawback of the generalized MP/SOFT method is that it requires generating a new coherent-state expansion of the time evolving state for each propagation step. The underlying computational task, however, can be trivially distributed on a parallel computer architecture. In addition, since the method is based on a perturbation expansion, the norm of the wave packet is not conserved and results need to be renormalized at any desired time according to the corresponding level of perturbation theory.

Relative to the original MP/SOFT formulation, which has already been shown to be accurate and efficient even in systems with many degrees of freedom,[38] the computational overhead necessary for including nonadiabatic effects is minor, specially when the approach is implemented according to the perturbation expansion to first-order accuracy. The computational overhead simply involves adiabatic propagation of the wave-packet components of each diabatic state and mixing the time-evolved wave packets at the end of each propagation time increment.

We have demonstrated the accuracy and efficiency of the generalized MP/SOFT propagation method as applied to the model systems introduced by Tully for testing simulations of dual curve-crossing dynamics with nonadiabatic couplings of different strengths, including a model of single avoided crossing, dual avoided crossing dynamics with manifested Stuckelberg oscillations, and a model of extended coupling with wave-packet reflection. Excellent agreement between MP/SOFT and benchmark grid-based calculations was demonstrated for all three model systems. Furthermore, results were obtained with rather efficient coherent state representations, often including fewer than 50 coherent states ($n \leqslant 50$).

Based on the benchmark calculations reported in this paper, we conclude that the method developed here is quite promising and should be applicable even to systems with many degrees of freedom and multiple-coupled potential-energy surfaces. This, however, remains to be demonstrated and is the subject of work in progress. Another aspect under current analysis involves exploring the implementation of flexible representations, in the spirit of recent works,[57,58] in an effort to reduce the coupling strength and, therefore, improve the numerical efficiency of the generalized MP/SOFT method in applications to model problems with strong couplings.

ACKNOWLEDGMENTS

One of the authors (V.S.B.) acknowledges supercomputer time from the National Energy Research Scientific Computing Center and financial support from Research Innovation Award RI0702 from Research Corporation, Petroleum Research Fund Award PRF 37789-G6 from the American Chemical Society, junior faculty award from the F. Warren Hellman Family, National Science Foundation (NSF) Career Program Award CHE-0345984, NSF Nanoscale Exploratory Research (NER) Award ECS-0404191, and start-up package funds from the Provost's office at Yale University. Another author (M.F.H.) acknowledges financial support from NSF Grant No. CHE-0203041.

[1] H. Nakamura, *Nonadiabatic Transitions: Concepts, Basic Theories, and Applications* (World Scientific, Singapore, 2002).
[2] A. Kondorskiy and H. Nakamura, J. Chem. Phys. **120**, 8937 (2004).
[3] D. Neuhauser, J. Chem. Phys. **100**, 9272 (1994).
[4] W. Zhu, J. Zhang, and D. Zhang, Chem. Phys. Lett. **292**, 46 (1998).
[5] G. Schatz, M. Fitzcharles, and L. Harding, Faraday Discuss. Chem. Soc. **84**, 359 (1987).
[6] D. Clary, J. Phys. Chem. **98**, 10678 (1994).
[7] R. Kosloff, Annu. Rev. Phys. Chem. **45**, 145 (1994).
[8] J. Fair, D. Schaefer, R. Kosloff, and D. Nesbitt, J. Chem. Phys. **116**, 1406 (2002).
[9] J. Echave and D. Clary, J. Chem. Phys. **100**, 402 (1994).
[10] H. Yu and J. Muckerman, J. Chem. Phys. **117**, 11139 (2002).
[11] M. Hernandez and D. Clary, J. Chem. Phys. **101**, 2779 (1994).
[12] D. Charlo and D. Clary, J. Chem. Phys. **117**, 1660 (2002).
[13] J. Bowman, J. Phys. Chem. A **102**, 3006 (1998).
[14] D. Xie, R. Chen, and H. Guo, J. Chem. Phys. **112**, 5263 (2000).
[15] S. Anderson, T. Park, and D. Neuhauser, Phys. Chem. Chem. Phys. **1**, 1343 (1999).
[16] M. D. Feit, J. A. Fleck, Jr., and A. Steiger, J. Comput. Phys. **47**, 412 (1982).
[17] M. D. Feit and J. A. Fleck, Jr., J. Chem. Phys. **78**, 301 (1983).
[18] D. Kosloff and R. Kosloff, J. Comput. Phys. **52**, 35 (1983).
[19] H. Tal-Ezer and R. Kosloff, J. Chem. Phys. **81**, 3967 (1984).
[20] T. Park and J. Light, J. Chem. Phys. **85**, 5870 (1986).
[21] R. Preston and J. Tully, J. Chem. Phys. **54**, 4297 (1971).
[22] J. Tully, J. Chem. Phys. **93**, 1061 (1990).
[23] R. B. Gerber, V. Buch, and M. A. Ratner, J. Chem. Phys. **77**, 3022 (1982).
[24] H. Meyer and W. H. Miller, J. Chem. Phys. **70**, 3214 (1979).
[25] X. Sun and W. H. Miller, J. Chem. Phys. **106**, 6346 (1997).
[26] M. Thoss and G. Stock, Phys. Rev. A **59**, 64 (1999).
[27] M. Herman and E. Kluk, Chem. Phys. **91**, 27 (1984).
[28] E. Kluk, M. Herman, and H. L. Davis, J. Chem. Phys. **84**, 326 (1986).
[29] G. Yang and M. Herman, J. Phys. Chem. B **105**, 6562 (2001).
[30] F. Webster, P. Rossky, and R. Friesner, Comput. Phys. Commun. **63**, 494 (1991).
[31] O. Prezhdo and P. Rossky, J. Chem. Phys. **107**, 825 (1997).
[32] D. Coker, in *Computer Simulation in Chemical Physics*, edited by M. Allen and D. Tildesley (Kluwer Academic, Dordrecht, 1993), pp. 315–377.
[33] S. Hammes-Schiffer, J. Chem. Phys. **105**, 2236 (1996).
[34] S. Hammes-Schiffer and J. Tully, J. Chem. Phys. **103**, 8528 (1995).

[35]N. Makri and W. H. Miller, J. Chem. Phys. **91**, 4026 (1989).
[36]Y. Wu and V. Batista, J. Chem. Phys. **118**, 6720 (2003).
[37]Y. Wu and V. Batista, J. Chem. Phys. **119**, 7606 (2003).
[38]Y. Wu and V. Batista, J. Chem. Phys. **121**, 1676 (2004).
[39]S. Mallat and Z. Zhang, IEEE Trans. Signal Process. **41**, 3397 (1993).
[40]E. Heller, Chem. Phys. Lett. **34**, 321 (1975).
[41]M. J. Davis and E. J. Heller, J. Chem. Phys. **71**, 3383 (1979).
[42]E. Heller, J. Chem. Phys. **75**, 2923 (1981).
[43]R. Coalson and M. Karplus, Chem. Phys. Lett. **90**, 301 (1982).
[44]S. Sawada, R. Heather, B. Jackson, and H. Metiu, Chem. Phys. Lett. **83**, 3009 (1985).
[45]K. G. Kay, J. Chem. Phys. **91**, 107 (1989).
[46]M. Ben-Nun and T. Martinez, J. Chem. Phys. **108**, 7244 (1998).
[47]K. Thompson and T. Martinez, J. Chem. Phys. **110**, 1376 (1999).
[48]M. Ben-Nun and T. Martinez, Adv. Chem. Phys. **121**, 439 (2002).
[49]D. V. Shalashilin and B. Jackson, Chem. Phys. Lett. **291**, 143 (1998).
[50]L. Andersson, J. Chem. Phys. **115**, 1158 (2001).
[51]D. Shalashilin and M. Child, J. Chem. Phys. **113**, 10028 (2000).
[52]D. Shalashilin and M. Child, J. Chem. Phys. **115**, 5367 (2001).
[53]M. Beck, A. Jackle, G. Worth, and H. Meyer, Phys. Rep. **324**, 1 (2000).
[54]X. Chen, Y. Wu, and V. Batista, J. Chem. Phys. (to be published).
[55]J. Burant and V. Batista, J. Chem. Phys. **116**, 2748 (2002).
[56]E. Nikitin, *Theory of Elementary Atomic and Molecular Processes in Gases* (Clarendon, Oxford, 1974).
[57]M. Herman, J. Chem. Phys. **111**, 10427 (1999).
[58]M. Herman, J. Chem. Phys. **110**, 4141 (1999).